Biophysical Chemistry, 44 (1992) 21–28
Elsevier Science Publishers B.V., Amsterdam

BIOCHE 01671

Dynamics of benzo[a]pyrene diol epoxide adducts in poly(dG-dC) · (dG-dC) studied by synchrotron excited fluorescence polarization anisotropy decay

A. Gräslund [a], S.K. Kim [b], S. Eriksson [b], B. Nordén [b] and B. Jernström [c]

[a] *Department of Medical Biochemistry and Biophysics, University of Umeå, S-901 87 Umeå (Sweden)*
[b] *Department of Physical Chemistry, Chalmers University of Technology, S-412 96 Gothenburg (Sweden)*
[c] *Department of Toxicology, Karolinska Institutet, S-104 01 Stockholm (Sweden)*

(Received 23 October 1991; accepted in revised form 4 March 1992)

Abstract

Time-resolved fluorescence studies have been performed on (+)-*anti*-7,8-dihydrodiol-9,10-epoxy-benzo[a]pyrene adducts in double-stranded poly(dG-dC) · (dG-dC). Part of the adduct population gives rise to excimer fluorescence. The heterogeneous fluorescence emission decay curves at 22°C could be resolved into three components with lifetimes: 0.4 ns, 3 ns and 24 ns for the total fluorescence (monomer and excimer emission), and 0.5 ns, 5 ns and 24 ns, respectively, for excimer emission alone. The relative amplitudes for the longer lifetimes were larger for the pure excimer population than for the mixed population. The fluorescence polarization anisotropy decay curves were resolved into two components of rotational correlation times: 0.4 ns and 25 ns for the total fluorescence and 0.3 ns and 33 ns for the excimer fluorescence. We interpret the two rotational correlation times to correspond to local motion of the adduct and segmental motion of the polynucleotide, respectively.

Keywords: Benzo[a]pyrene diol epoxide; Poly(dG-dC)·(dG-dC); Synchrotron radiation; Fluorescence lifetimes; Anisotropy decay

1. Introduction

Benzo[a]pyrene diol epoxides are considered to be the ultimate carcinogens of benzo[a]pyrene (BP). (+)-*anti*-7,8-dihydrodiol-9,10-epoxy-benzo [a]pyrene (BPDE) is the most tumorigenic one of four possible stereoisomers. It binds covalently with high specificity to guanine in double stranded DNA. Previous optical studies have revealed a significant spectral heterogeneity of these adducts. The plane of BPDE is on an average localized at a 20° angle with the helix axis, most likely in the minor groove of DNA. The DNA structure is probably locally disordered or bent at the site of the adduct [1–4].

When BPDE is bound to poly (dG-dC) · (dG-dC), one part of the adduct population can give rise to excimer fluorescence [5,6]. In the present investigation we have studied the fluorescence emission decay and polarization anisotropy decay

Correspondence to: Professor Astrid Gräslund, Department of Medical Biochemistry and Biophysics, University of Umeå, S-901 87 Umeå, Sweden.

properties in experiments where we have tried to select fluorescence from monomer or excimer populations of the BPDE adducts, using synchrotron light as the source of excitation. The evaluation of the fluorescence polarization anisotropy decay curves gives for the first time dynamic information on the time scale of motion of the carcinogenic BPDE adducts in a nucleic acid.

2. Materials and methods

(+)-*anti*-BPDE was reacted with poly(dG-dC)·(dG-dC) as previously described [6] and followed by extensive dialysis against 1 m*M* Na cacodylate buffer, pH 7.0, 10 m*M* NaCl. The concentration of the poly(dG-dC)·(dG-dC) was measured spectrophotometrically at 255 nm and was adjusted to be in the range 0.12–0.18 m*M* (based on an absorption coefficient $\epsilon_{255} = 8{,}400$ M^{-1} cm^{-1} per nucleotide unit [7]). A typical modification ratio (BPDE per nucleotide) was 0.5%, judged from the optical absorption at 345 nm of the BPDE adduct ($\epsilon_{345} = 29{,}000$ M^{-1} cm^{-1} [8]). A 0.2-ml sample was placed in a 5 mm × 5 mm quartz cuvette.

Fluorescence and polarization anisotropy decay processes were studied at the beamline for time-resolved spectroscopy at the MAX-synchrotron laboratory at Lund, Sweden [9–11]. The synchrotron operating in the single bunch mode had a light pulse of Gaussian shape with a variance of 60 ps. A monochromator with a band width of 9 nm was used on the excitation side, whereas edge filters (high wavelength pass) from Schott-Jena were used on the emission side for optimum fluorescence signal intensity. Polarized and unpolarized components of the decay were measured by the time-correlated single photon counting technique using a microchannel plate detector.

Four different data sets were collected [12,13]: synchrotron light, dark current, $I_\perp$ and I_m, where $I_\perp$ is the perpendicular intensity and I_m is the magic angle intensity relative to the polarization of the exciting light pulse. The decay was followed for 40 ns and the synchrotron pulses were repeated every 108 ns. The time spent on each measurement was typically one hour, cycling through collection in the different data sets every 80 s. All measurements were performed in the presence of 0.5 *M* acrylamide to minimize the fluorescence contribution from contaminating benzo[a]pyrene-7,8,9,10-tetraol, a highly fluorescent hydrolysis product of BPDE or its polynucleotide adduct [14].

The analysis of the data is based on the concept of discrete fluorescence decay and polarization anistropy decay components and was described in [13]. The important features are summarized here.

Fluorescence decay curves $I_m(t)$ were described as a sum of discrete exponential components:

$$I_m(t) = \sum_i \alpha_i \exp(-t/\tau_i), \tag{1}$$

where τ_i is a fluorescence lifetime and α_i its amplitude. The χ^2 statistical analysis of the calculated $I_m(t)$ convoluted with the synchrotron pulse relative to the experimental curve is a measure of the systematic error in the "best fitting" model curve. With a χ^2 value close to 1, the deviations between the model and the experimental result are mainly due to noise.

The decay of fluorescence polarization anistropy of the system is a function of the rotational correlation times as well as the fluorescence decay times. The rotational correlation times ρ_i were evaluated under the assumption that each rotational component is associated with all decay components (previously determined) through

$$\frac{I_\perp(t)}{I_m(t)} = 1 - \frac{\left(\sum_i \beta_i \exp(-t/\rho_i)\right)\left(\sum_j \alpha_j \exp(-t/\tau_j)\right)}{\sum_j \alpha_j \exp(-t/\tau_j)} \tag{2}$$

β_i is the zero-time anisotropy for component i and ρ_i is the corresponding rotational correlation

time. In the second term of this expression, both nominator and denominator are convoluted with the synchrotron light pulse shape to obtain the entity that (after subtraction from 1) is fitted to the experimentally determined ratio $I_{\perp}(t)/I_{m}(t)$. If the detector sensitivity difference in the $I_{\perp}$ and I_{m} components is properly compensated for, $I_{\perp}(t)/I_{m}(t)$ should approach 1 at longer times.

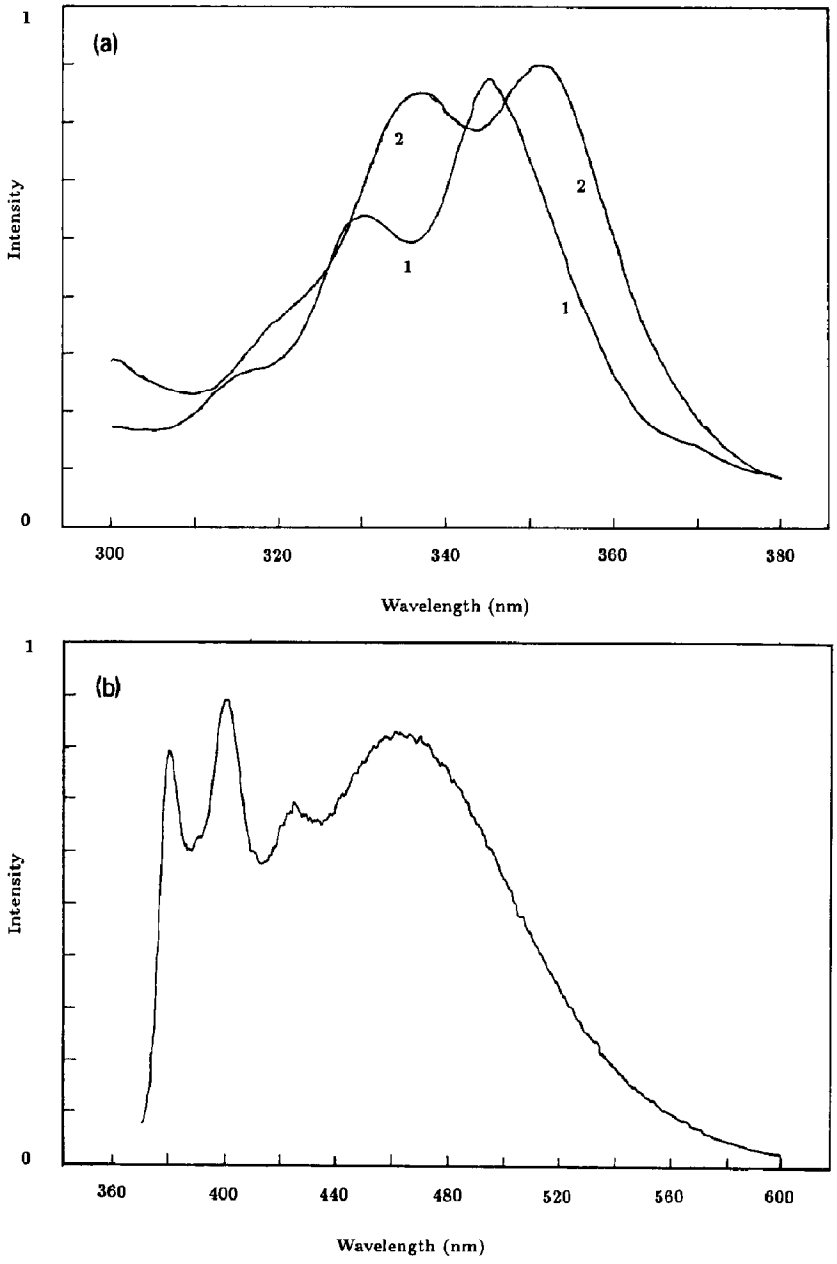

Fig. 1. Fluorescence excitation (a) and emission spectra (b) of (+)-*anti*-BPDE-poly(dG-dC)·(dG-dC) adducts in 1 m*M* sodium cacodylate buffer, 10 m*M* NaCl, pH 7.0 at 22°C. (a) Excitation spectra recorded with emission wavelength 400 nm (1) or 470 nm (2). (b) Emission spectrum after excitation at 345 nm.

3. Results and discussion

The monomer and excimer components of the fluorescence spectra of the (+)-*anti*-BBDE-polynucleotide adducts in poly(dG-dC)·(dG-dC) are distinguished by different spectral characteristics [6]. Figure 1 and Table 1 show the main features of the excitation and emission spectra of the two components. For the partly resolved vibrational components of the monomer emission the

Table 1

Excitation and emission maxima of monomeric and excimeric fluorescence of (+)-*anti*-BPDE adducts in poly(dG-dC)·(dG-dC) [4]

Fluorescence component	Excitation maxima (nm)	Emission maxima (nm)
Monomer	316, 330, 345	380, 400, 420
Excimer	319 [a], 334, 352	462

[a] Shoulder.

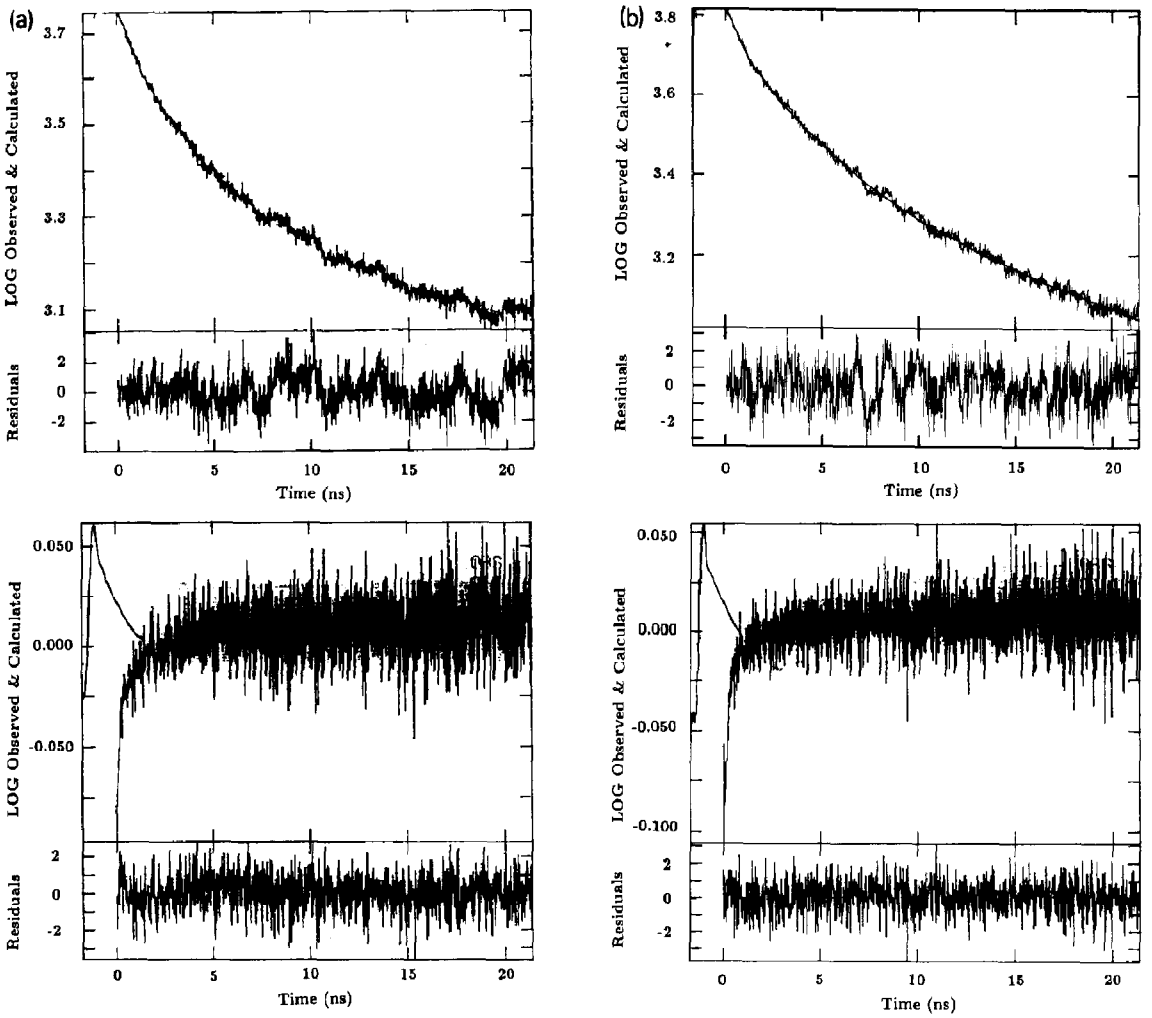

Fig. 2. Fluorescence emission decay (upper frame) and polarization anisotropy decay (lower frame) curves of BPDE adducts in poly-(dG-dC)·(dG-dC), in 1 m*M* sodium cacodylate buffer, 10 m*M* NaCl, pH 7.0 at 22°C. The fluorescence was excited at (a) 346 nm or (b) 352 nm and recorded with a high pass filter with an edge at 360 nm or 430 nm, respectively. The plotted quantity in the anisotropy curves is log ($I_{\perp}$ / I_{m}). Also indicated in the lower frame is the shape of the synchrotron light pulse in arbitrary logarithmic scale. The residual deviations between experimental and theoretical curves are indicated.

linewidth at half height is about 15 nm, whereas the unstructured excimer emission has a linewidth at half height of about 120 nm. If fluorescence emission is recorded at wavelengths longer than 430 nm, it will arise mainly from the excimeric component. There was, however, no simple way to observe only the monomeric component in the present experiments. The best discrimination we could achieve was to excite around 350 nm and record all emission utilizing either a 360 nm or 430 nm cut off filter. The former contains both monomer and excimer components and the latter is dominated by excimer fluorescence. The light intensity was too low to allow the use of a monochromator on the emission side when observing the polarization anisotropy decay.

Fluorescence polarization anisotropy (FPA) was measured as $I_\perp/I_m$, where I_m is the magic angle intensity and $I_\perp$ is the perpendicular intensity relative to the polarization of the exciting light pulse. Fluorescence (I_m) and polarization anisotropy decay curves were obtained with excitation and emission parameters corresponding to a mixture of monomer and excimer or to mainly excimer fluorescence (Fig. 2). It should be noted that in the representation used here for polarization anisotropy decay, the fitted quantity is log $(I_\perp/I_m)$, where $I_\perp$ and I_m are the direct observables. At times close to zero this quantity should be negative $(I_\perp/I_m < 1)$ and should approach a value close to zero $(I_\perp/I_m = 1)$ at long times, as is obviously the case for the curves shown in Fig. 2.

The decay curves were evaluated as previously described [12,13]. The rotational correlation times were evaluated from $I_\perp/I_m$ using the theoretical fluorescence decay parameters from the I_m decay. The results in terms of relative amplitudes, fluorescence decay times and rotational correlation times are shown in Table 2. For the fluorescence decay curves at least three components were needed to yield reasonable fits (χ^2 close to 1). Two exponential components were generally sufficient to fit the polarization anisotropy decay curves.

The measurements were repeated several times using different samples with somewhat different adduct formation ratios. The results were repro-

Table 2

Fluorescence decay and anisotropy decay parameters of (+) -*anti*-BPDE adducts in poly(dG-dC)·(dG-dC) in 1 m*M* Na-cacodylate buffer, pH 7.0, 10 m*M* NaCl, at 22°C. α_i and τ_i are amplitudes and fluorescence decay times, respectively, and β_i and ρ_i are amplitudes and rotational correlation times, respectively. The amplitudes have been normalized so that their sum adds up to 1

Emitting species	Fluorescence decay parameters								
	λ_{ex} (nm)	λ_{em} (nm)	α_1	τ_1 (ns)	α_2	τ_2 (ns)	α_3	τ_3 (ns)	χ^2
BPDE monomer	346	> 375	0.70	0.43	0.25	2.40	0.058	14.4	1.03
+ excimer	346	> 385	0.68	0.46	0.19	3.15	0.13	20.1	1.18
	346	> 375	0.65	0.49	0.22	2.89	0.14	19.8	1.39
	345	> 375	0.47	0.41	0.33	3.49	0.21	41.3	1.65
BPDE excimer	354	> 475	0.33	0.54	0.32	8.06	0.35	27.2	0.96
	346	> 455	0.61	0.48	0.44	4.74	0.25	22.7	1.05
	345	> 435	0.46	0.37	0.31	3.58	0.23	23.4	1
	Polarization anisotropy decay parameters								
	λ_{ex} (nm)	λ_{em} (nm)	β_1	ρ_1 (ns)	β_2	ρ_2 (ns)	χ^2		
BPDE monomer	345	> 375	0.64	0.53	0.36	33	1.10		
+ excimer	345	> 375	0.78	0.29	0.22	17	1.11		
BPDE excimer	345	> 435	0.79	0.23	0.21	33	0.97		
	350	> 435	0.49	0.36	0.51	33	1.09		

ducible but with large uncertainties, as shown in Table 2 where the results of several separate measurements are reported. Calculated mean values for the lifetimes are 0.4 ns, 3 ns, and 24 ns for the monomer/excimer fluorescence and 0.5 ns, 5 ns and 24 ns for the excimer fluorescence, respectively. For the rotational correlation times the mean values are 0.4 ns and 25 ns for the monomer/excimer population and 0.3 ns and 33 ns for the excimer population, respectively.

Judging from the reproducibility of the results of the different measurements, the uncertainty in the lifetime parameters is about 20%, whereas it is as large as 50% in the anisotropy decay parameters. Three important reasons for these large uncertainties are: (1) the rather low light intensity which leads to noisy decay curves and necessitates measurement times on the order of one hour, during which time the sample may decompose to different extents in the light beam (the fluorescence intensity is of course a result of both the exciting light intensity as well as of fluorescence quantum yield, which is rather low for most BPDE–DNA adducts [1,15]); (2) a certain inhomogeneity in the freshly prepared samples (although chemically homogeneous, with most BPDE adducts attached to N-2 of guanine, the monomer–excimer distribution seems to vary somewhat between preparations, probably due to different rates of formation as well as loss of adducts); (3) the current shape of the synchrotron pulse, which varies to some extent between injections to the ring.

The results show that the BPDE populations yielding either the mixed monomer/excimer or the excimer fluorescence appear heterogeneous. The BPDE population yielding excimer fluorescence has an overall slower fluorescence decay process partly because of longer decay times but mainly because of larger amplitudes for the longer decay times (cf. refs. [6,14]). To ensure that the longest lifetime component is not significantly affected by a variable amount of fluorescence from free BP-7,8,9,10-tetraol from hydrolyzed BPDE or its polynucleotide adducts [14], we added acrylamide acting as a fluorescence quencher to the solvent. This may at least in part explain the shorter lifetimes observed in this study compared to [6]. Processes with lifetimes on the order of 100 ns are not well observable in the present experiments since the synchrotron pulse was repeated every 108 ns and the decay was followed during 40 ns.

The two exponential components required to describe the polarization anisotropy decay were about 20–30 ns and 0.5 ns, respectively. A straightforward interpretation is that the longer one is associated with the motion of a whole polynucleotide segment, whereas the shorter one is associated with local motion of the BPDE adduct. Obviously the time scales for the two types of depolarizing motion is not significantly different for the adduct populations yielding either the mixed monomeric/excimeric or the excimeric emission of BPDE.

The sums of the absolute values of the zero-time amplitudes of the polarization decay components are about 0.1–0.2 for both populations. These sums should reflect the steady-state anisotropies in the system, and would have a maximum value of 0.4 if the absorbing and emitting transition moments were parallel [16]. A previous steady-state measurement on immobilized BPT gave a result of 0.17 for the steady-state anisotropy [6]. Considering the relatively large uncertainties involved in the anisotropy decay measurements, the agreement between our $\Sigma_i \beta_i$ and the steady-state anisotropy is good and indicates that most of the motion is accounted for in our measurements.

The relative size of the amplitude for the longer rotational correlation time describes the anisotropy remaining in the system after the rapid motion has completed its averaging. It is therefore dependent on the angular displacement related to the rapid motion through $\cos^2\gamma = (2\beta_2 + 1)/3$, where $\cos^2\gamma$ is an average value, and γ is the angular displacement characteristic of the rapid motion [17]. For both populations the amplitude for the longer rotational correlation time is shorter than or similar to the amplitude of the smaller one. The absolute values of β_2 are of the order of 0.05, which gives rise to an estimated value of γ of about 50°. The results are based on the simple model in which both components of depolarizing motion are equally connected to all

three decay species, which may be an oversimplification.

Studies on ethidium bromide intercalated in calf thymus DNA fragments of different lengths have indicated a rotational correlation time for a "twisting" motion of 5–10 ns for a fragment > 100 base pairs [18]. This time window for the segmental polynucleotide motion is in approximate agreement with the longer rotational correlation time observed by us for the poly(dG-dC)·(dG-dC) adduct. The subnanosecond motion of the BPDE adduct is reasonable for local motion of the adduct relative to the polynucleotide. It is on a comparable timescale with that of a fluorescent base analog, 2-aminopurine, when it is incorporated in an oligonucleotide duplex and base-paired with thymine [19].

The detailed understanding of the origin of the excimer fluorescence component from BPDE in poly(dG-dC)·(dG-dC) is still lacking along with its potential implications for the biological (carcinogenic) effect of BPDE. One question is whether the excimer is really an excimer between two pyrene-derived fluorophores, or whether the unstructured emission arises from an exciplex, i.e. a complex between a pyrene aromatic system and a DNA base, presumably guanine [14]. We reacted the dinucleotide $(dG)_2$ with BPDE and found no indication of excimer emission from the adducts formed in this case (data not shown). Although not conclusive, this experiment shows that only the presence of guanine bases in the vicinity of the BPDE adduct is not sufficient to induce excimer fluorescence, and therefore is an argument in favour of excimer rather than exciplex emission.

Another important question is whether BPDE binding to polynucleotides is cooperative. If it is, the cooperativity may be connected to the appearance of excimers in poly(dG-dC)·(dG-dC). A third question concerns DNA sequence specificity for BPDE adduct formation. Double-stranded alternating GC sequences are obviously good substrates *in vitro*. A preferred sequence may be very short, e.g. GC/CG or GCG/CGC. If there is also cooperative binding to closely spaced G's on the same or opposite strands, a result may be the observed favoured excimer formation in alternating poly(dG-dC)·(dG-dC). Excimer fluorescence in DNA sequences may then be a marker for the presence of extensively modified and structurally changed stretches of DNA. However, although BPDE binding sites have been found to be markedly non-randomly distributed in a chicken β-globin gene, no simple correlation to guanine density along the gene has been observed [20].

In conclusion, the presented studies on the fluorescence decay and polarization decay processes in BPDE–poly(dG-dC)·(dG-dC) adducts reveal heterogeneous emission systems with three lifetimes and two rotational correlation times, the latter probably corresponding to local motion of the chromophore and segmental motion of the polynucleotide, respectively. The population of the adducts giving rise to excimer emission in many respects appears similar to that giving rise to the mixed monomer/excimer emission. One apparent difference between the two populations is, however, that the excimer-yielding population to a higher extent exhibits longer fluorescence lifetimes (smaller amplitude for the shortest lifetime).

Acknowledgements

We wish to thank Dr. R. Rigler for help and advice about using the beamline for time-resolved spectroscopy at the MAX-synchrotron laboratory, Dr. L. Nilsson for advice about the use of the data evaluation system, and Mr. J. Roslund for expert technical assistance. This study was supported by grants from the Swedish Work Environment Fund, the Swedish Cancer Society and the Swedish Natural Science Research Council.

References

1 A. Gräslund and B. Jernström, Q. Rev. Biophys. 22 (1989) 1.
2 M. Eriksson, B. Nordén, B. Jernström and A. Gräslund, Biochemistry 27 (1988) 1213.
3 N.E. Geacintov, M. Cosman, V. Ibanez, S.S. Birke and C.E. Swenberg, in: Molecular basis of specificity in nucleic

acid-drug interactions, eds. B. Pullman and J. Jortner (Kluwer Acad. Publ., Dordrecht, 1990) pp. 433–450.
4 B. Singh, B.E. Hingerty, U.C. Singh, J.P. Greenberg, N.E. Geacintov and S. Broyde, Cancer Res. 51 (1991) 3482.
5 M. Eriksson, B. Nordén, B. Jernström, A. Gräslund and P-O. Lycksell, J. Chem. Soc. Chem. Commun. (1988) 211.
6 M. Eriksson, S. Eriksson, B. Jernström, B. Nordén and A. Gräslund, Biopolymers 29 (1990) 1249.
7 R.D. Wells, J.E. Larson, R.C. Grant, B.E. Shortle and C.R. Cantor, J. Mol. Biol. 54 (1970) 465.
8 P. Pulkrabek, S. Leffler, I.B. Weinstein and D. Grunberger, Biochemistry 16 (1977) 3127.
9 R. Rigler, F. Claesens and G. Lomakka, in: Ultrafast Phenomena IV (Springer Series in Chemical Physics 38), eds. D.H. Auston and K.B. Eisenthal (Springer Verlag, Berlin, 1984) pp. 472–476.
10 R. Rigler, O. Kristensen, J. Roslund, P. Thyberg, K. Oba and M. Eriksson, Physica Scripta T17 (1987) 204.
11 R. Rigler, J. Roslund and S. Forsén, Eur. J. Biochem. 188 (1990) 541.
12 F. Claesens and R. Rigler, Eur. J. Biophys. 13 (1986) 331.
13 A.D. MacKerell Jr., R. Rigler, L. Nilsson, U. Hahn and W. Saenger, Biophys. Chem. 26 (1987) 247.
14 S.K. Kim, N.E. Geacintov, D. Zinger and J.C. Sutherland, in: Brookhaven Symposium in Biology, No. 35, Synchrotron radiation in structural biology (Upton, New York, NY, 1989) p. 187.
15 L. Margulis, P.F. Pluzhnikov, B. Mao, V.A. Kuzmin, Y.J. Chang, T.W. Scott and N.E. Geacintov, Chem. Phys. Lett. (1992) in press.
16 J.R. Lakowicz, Principles of fluorescence spectroscopy (Plenum Press, New York, NY, 1983) pp. 156–157.
17 J.R. Lakowicz, Principles of fluorescence spectroscopy, (Plenum Press, New York, NY, 1983) p. 168.
18 T. Härd and D.R. Kearns, Nucleic Acids Res. 14 (1986) 3945.
19 T.M. Nordlund, S. Andersson, L. Nilsson, R. Rigler, A. Gräslund and L.M. McLaughlin, Biochemistry 28 (1989) 9095.
20 T.C. Boles and M.E. Hogan, Proc. Natl. Acad. Sci. USA 81 (1984) 5623.